LOCAL FIELD ENHANCEMENT NEAR SPHERICAL NANOPARTICLES IN ABSORBING MEDIA

**R. A. Dynich, A. N. Ponyavina,
and V. V. Filippov**[*]

UDC 535.343:541.1

It is shown by numerical simulation that the enhancement of the field near metallic nanoparticles is most significant in the transparency region of the matrix material and falls off as the absorption coefficient rises. In an absorbing matrix medium this leads both to an increase in the fraction of energy absorbed by the matrix material and to a substantial transformation in its spectral distribution. This is illustrated for the case of copper phthalocyanine with silver nanoparticles. By choosing the size of the introduced plasmon nanoparticles it is possible to enhance the absorption in the visible for the materials used in solar cells and thereby increase their energy efficiency.

Keywords: *local field intensity, enhanced absorption, silver nanoparticles, copper phthalocyanine.*

Introduction. When plasmonic nanoparticles are present in a medium, surface plasmon absorption bands form and cause a substantial enhancement in the local electromagnetic field in the spectral region of the plasmon resonance [1–4]. The surface plasmon resonance responsible for the enhancement in the local field is primarily a characteristic of the metal from which the nanoparticles are made. However, certain features of this effect are determined by the sizes and shapes of the nanoparticles, and their organization (nanostructure), but also depend on the optical properties of the medium in which the nanoparticles are embedded. By changing the shape and size of the nanoparticles it is relatively easy to control the characteristics of the surface plasmon resonance.

The possibility of local field enhancement in a medium turns out to be attractive for applications in photovoltaic solar cells, since an enhanced field raises the fraction of energy absorbed in the medium, which is proportional to the local field intensity. This is one of the concepts now under rapid development for raising the conversion efficiency for solar energy, both for cells with traditional semiconductors (silicon [5], gallium arsenide [6]) and thin film cells based on organic semiconductors [7].

Up to now primary attention has been devoted to the features of the plasmon resonance and the local field enhancement in transparent media. However, absorption in a matrix material does affect the efficiency with which light is scattered [8–11]. Thus, one should expect changes in both the intensity and the character of the localization of "hot spots," and a transformation in the resulting absorption spectrum of the composite medium. In addition, with regard to absorbing media (and highly absorbing materials are used in photovoltaic cells), the presence of an additional spatial dependence of the wave field has a significant effect on the procedure for calculating and characterizing light scattering [12–15].

Numerical Simulation Technique. The field near the surface of a spherical particle was determined by an approach based on Mie's theory. Our own computer program developed for the case in which the surrounding medium is absorbing was used. The near field distribution was described with the aid of the near zone scattering efficiency factor Q_{NF} [2]. The factor Q_{NF} characterizes the total enhancement in the local field intensity over the surface of radius R (the centers of the nanoparticle and of the sphere of integration coincide with the coordinate origin) and for nonabsorbing media it is given by

---

[*]To whom correspondence should be addressed.

$$Q_{\mathrm{NF}} = \frac{R^2}{\pi a^2 I_0} \int\limits_0^{2\pi} \int\limits_0^{\pi} \mathbf{E}_s \mathbf{E}_s^* \sin\theta \, d\theta \, d\varphi \big|_{R=a}, \tag{1}$$

where $\mathbf{E}_s$ is the electric field of the scattered wave in the near zone, I_0 is the intensity of the incident light, and * denotes the complex conjugate.

As the radius R is increased the integration yields a lower value of Q_{NF} and it approaches the scattering efficiency factor Q_{sc}. An exact calculation of Q_{NF} invoking Mie's theory can be carried using the following expression [2, 3]:

$$Q_{\mathrm{NF}} = \frac{2R^2}{a^2} \sum_{n=1}^{\infty} \left\{ |a_n|^2 \left[(n+1) \, |h_{n-1}|^2 + n \, |h_{n+1}|^2 \right] + (2n+1) \, |b_n|^2 \, |h_n|^2 \right\}, \tag{2}$$

where a_n and b_n are the scattering coefficients of the sphere and h_n is the spherical Hankel function of the first kind of order n. In calculating Q_{NF} it was assumed that the intensity $I_0 = \mathrm{const}$ and, therefore, that the flux of radiation incident on the particle is $I_0 \pi a^2$.

In an absorbing medium there is a reduction in the amplitude of the field along the (direction of) propagation of a light wave, so that the intensity of the incident light at points on the surface of the particle will vary. In this case the flux of the radiation incident on the particle is [8]

$$W_0 = \frac{2\pi a^2}{\eta^2} I_0 \left[1 + e^{\eta} (\eta - 1) \right], \tag{3}$$

where $\eta = 4\pi a m_i / \lambda_0$; $I_0 = m_r |E_0^2| / 2c\mu$; m_r and m_i are the real and imaginary parts of the complex refractive index of the medium; λ_0 is the vacuum wavelength of the light incident on the particle; c is the speed of light in a vacuum; and, μ is the absolute magnetic permeability of the medium. At the origin of the coordinate system the electric field strength of the incident wave takes on a certain value denoted by E_0. In the limit of $m_i \rightarrow 0$, we obtain $W_0 = 2\pi a^2 I_0$.

The attenuation of the intensity of the incident light beam owing to absorption in the particle and scattering on it is determined by the attenuation efficiency factor Q_{ext}. The following expression has been obtained for calculating it in an absorbing matrix [15]:

$$Q_{\mathrm{ext}} = \frac{4m_i^2}{m_r \left[1 + e^{\eta} (\eta - 1) \right]}$$

$$\times \mathrm{Re} \left\{ \frac{1}{m_i - im_r} \sum_{n=1}^{\infty} \left[(2n+1) \left(\psi_n^* \psi_n' - \psi_n \psi_n'^* + b_n \psi_n'^* \xi_n + b_n^* \psi_n \xi_n'^* - a_n \psi_n^* \xi_n' - a_n^* \psi_n' \xi_n^* \right) \right] \right\}, \tag{4}$$

where $\psi_n, \xi_n, \psi_n', \xi_n'$ are the Riccati-Bessel functions and their derivatives.

For a spherical particle located in an absorbing medium, the formula for calculating Q_{NF} can be written in the form

$$Q_{\mathrm{NF}} = \frac{(4\pi m_i R)^2}{\lambda^2 \left[1 + e^{\eta} (\eta - 1) \right]} \sum_{n=1}^{\infty} \left\{ |a_n|^2 \left[(n+1) \, |h_{n-1}|^2 + n \, |h_{n+1}|^2 \right] + (2n+1) \, |b_n|^2 \, |h_n|^2 \right\}. \tag{5}$$

The calculations were done using Eqs. (4) and (5), both including the size dependence for the optical constants of silver and taking this dependence into account through a model with a limit on the electron mean free path [1].

Results. This analysis is for spherical silver nanoparticles with radii of 1–50 nm. The optical constants for silver are taken from [16]. Figure 1 illustrates the effect of absorption by the matrix on the spectral dependence of the attenuation and scattering efficiency factors in the near zone of silver nanoparticles. This shows that increased absorp-
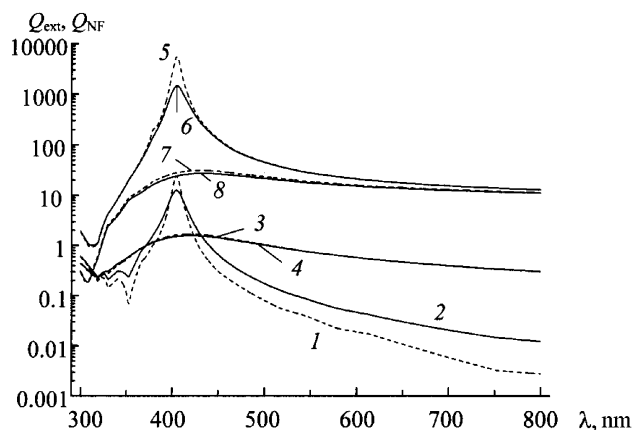
Fig. 1. The spectral variation in the efficiency factors for attenuation Q_{ext} (1–4) and scattering Q_{NF} (5–8) in the near zone by 10-nm-radius silver nanoparticles embedded in a nonabsorbing matrix with a refractive index of 1.5 (1, 2, 5, 6) and in a matrix with a complex refractive index of 1.5 + 0.5i (3, 4, 7, 8); 1, 3, 5, 7 and 2, 4, 6, 8 correspond to calculations which neglect and include, respectively, the size dependence of the refractive index of spherical silver nanoparticles.

tion by the matrix in which the silver nanoparticles are embedded causes a substantial broadening of the surface plasmon absorption resonances and a drop in their maximum intensity. At that same time, there is a significant reduction in the near field enhancement efficiency, which shows up especially strongly near the peak in the surface plasmon absorption resonance. The size dependence of the optical constants of silver nanoparticles has a significant effect on the spectra of Q_{ext} and Q_{NF} of nanoparticles in a transparent matrix while there is essentially no effect in the spectra of Q_{ext} and Q_{NF} in a highly absorbing matrix, where the surface plasmon absorption resonance is weak.

Since a substantial enhancement of the field by silver nanoparticles is observed near the plasmon resonance frequency, the distribution of the near field has been calculated for this frequency. The field distribution inside and outside a particle is visualized using two dimensional plots. An analysis of these plots shows that the topology of the distribution of the field enhancement regions is essentially invariable for small particles and undergoes a transformation as the particle size increases. For small spherical particles (a < 10 nm) the field patterns are typically symmetric inside and outside the particle with respect to all three main cross section planes passing through the center of the particle [4]. The regions with the highest field amplitudes, the "hot spots," are concentrated predominantly on the particle surface near its diametrally opposite poles along the polarization vector of the incident light. with increasing distance from the particle surface, the field falls off rapidly. As the particle radius is increased, the "hot spots" shift in the propagation direction of the incident wave, while remaining on the particle surface.

The actual materials used as matrices for metallic nanoparticles usually have dispersion in their complex refractive index. The visible spectra of these materials include both absorption bands and regions of high transparency. This makes an analysis of the field enhancement near the surface of metallic nanoparticles more difficult and requires that each specific matrix material be examined individually. We shall consider the case of Ag nanoparticles embedded in films of copper phthalocyanine (CuPc). These materials were chosen because they are used extensively in photovoltaic cells (CuPc) and plasmonics (Ag).

Some spectral dependences of the attenuation and scattering efficiency factors Q_{ext} and Q_{NF} in the near zone for silver nanoparticles in a CuPc matrix are shown in Fig. 2. The sizes of the nanoparticles were varied over a wide range, from 1 to 50 nm. Recall that CuPc absorbs strong in the UV (with a maximum near 370 nm) and has two absorption peaks in the visible, at 624 nm (m_i = 0.78) and, less intense, at 690 nm [17]. In the wavelength interval 400–540 nm, CuPc is more transparent, with a maximum transparency at λ = 500 nm.

It can be seen in Fig. 2 that both Q_{ext} and Q_{NF} increase in the transparency region of the matrix. Thus, for example, for Ag nanoparticles with a radius of 1 nm, at λ = 500 nm, where the imaginary part of the refractive index

707
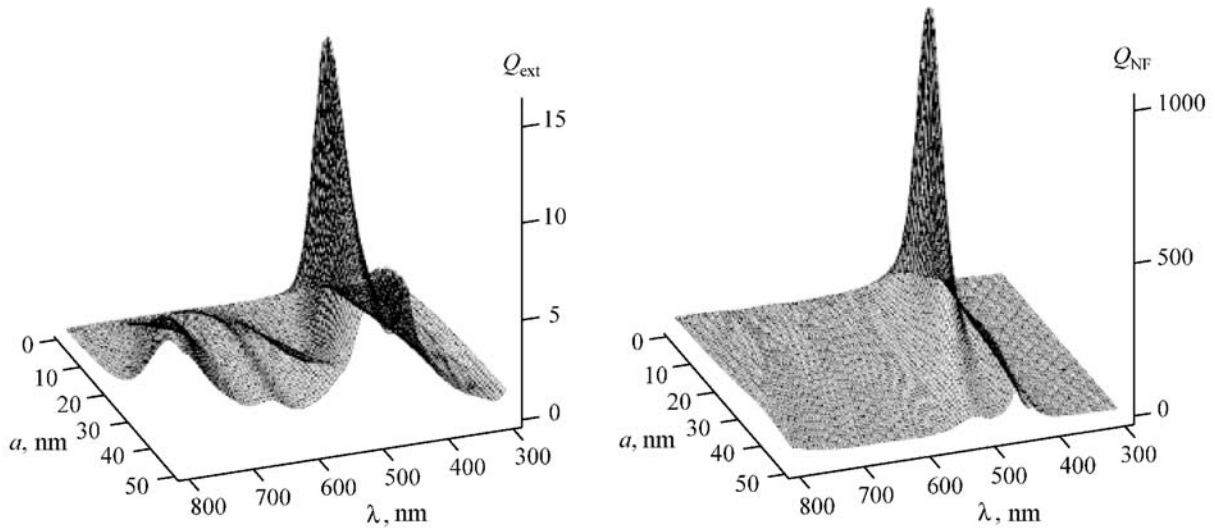
Fig. 2. Q_{ext} and Q_{NF} as functions of the radius a of a silver nanoparticle and the wavelength λ of the incident light taking particle size effects into account; the matrix is copper phthalocyanine.

of CuPc is minimal ($m_i = 0.0047$), $Q_{\text{NF}} = 32.8$. At the same time, in the region where the matrix has maximal absorption ($m_i = 0.78$) at $\lambda = 624$ nm, $Q_{\text{NF}} = 10.4$. This trend is maintained as the particle radius is increased. Q_{NF} reaches its maximum values for particles with a radius of ≈ 10 nm (for $\lambda_0 = 446$ nm, $Q_{\text{NF}} = 1016$). It is interesting to note that when the sizes of the nanoparticles are increased further, there are two spectral regions with high Q_{NF}. This corresponds to the development of a mode structure in the plasmon resonance at large nanoparticles [1].

Recall that Q_{NF} characterizes the efficiency with which a spherical particle transforms the field intensity of an incident wave into the intensity of the field in the zone near the particle. For a given wavelength and, therefore, for a certain value of m_i the absorption in the CuPc matrix will rise as the field intensity increases. This means that, thanks to the introduction of plasmonic nanoparticles, the efficiency of absorption enhancement in CuPc, which can be characterized by the product $Q_{\text{NF}}m_i$, may turn out to be comparable within the transparency regions of the matrix to the analogous quantity for the spectral regions where the matrix absorption is large.

In fact, as Fig. 3 shows, the spectral variation in $Q_{\text{NF}}m_i$ differs substantially from that of m_i. For 10-nm-radius silver nanoparticles the spectral variation of $Q_{\text{NF}}m_i$ is characterized by the presence of three maxima, two of which (at long wavelengths) are determined by the peaks in the absorption coefficient of CuPc, while the third (at short wavelengths) is determined by the peak scattering efficiency Q_{NF} in the near zone. Thus, introducing metallic nanoparticles both increases the absorption of CuPc films and transforms the spectral dependence of the absorption.

It is also important to note that the way the spectral variation in the absorption of CuPc is transformed is determined by the chosen size of the silver nanoparticles. This is related to the size dependence of the wavelength of the surface plasmon absorption resonance and the resulting size dependence for the spectrum of Q_{NF}. The calculations show that increasing the size of silver nanoparticles embedded a CuPc matrix causes a shift in the peak of Q_{NF} to longer wavelengths.

Increasing the radius R of the sphere of integration reduces the amplitude $|\mathbf{E}_s|$ of the scattered field and, thereby, lowers Q_{NF}. Thus, for a silver particle with $a = 10$ nm, at a distance a from its surface, i.e., at $R = 2a$, Q_{NF} is smaller by a factor of ≈ 15, regardless of wavelength. At a distance of $R = 3a$, the factor Q_{NF} becomes extremely small, and is ≈ 70 times smaller than Q_{NF} at the particle surface. A similar tendency shows up in the case of the product $Q_{\text{NF}}m_i$ (Fig. 4).

The efficiency with which the absorption of the matrix is increased by introducing nanoparticles is most fully characterized by the integrated effect over the entire spectrum. To estimate this efficiency we introduce the quantity
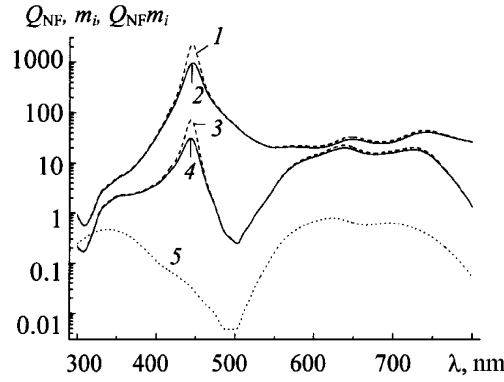
Fig. 3. Spectral variations in Q_{NF} (1, 2), m_i (5), and the product $Q_{NF}m_i$ (3, 4) for silver nanoparticles with a radius $a = 10$ nm neglecting (1, 3) and including (2, 4) particle size effects.
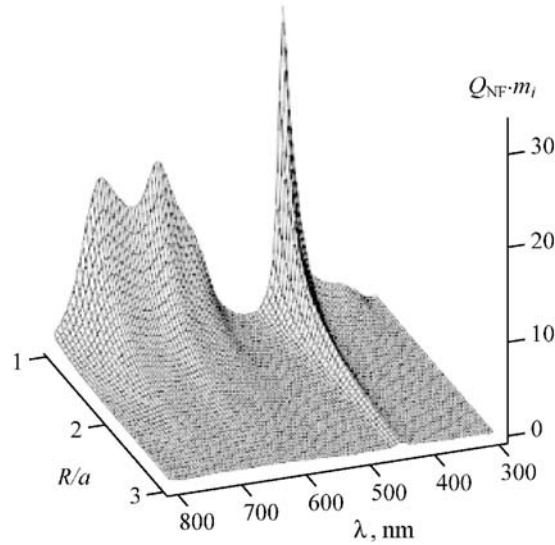

Fig. 4. A three dimensional plot of the product $Q_{NF}m_i$ as a function of λ and R/a for a silver nanoparticle with a radius $a = 10$ nm taking particle size effects into account.

$$A^R = \frac{\int Q_{NF}^R (\lambda) \, m_i (\lambda) \, d\lambda}{\int m_i (\lambda) \, d\lambda}, \tag{6}$$

which describes the field enhancement at a distance R from the center of a nanoparticle. By subsequent integration of this quantity with respect to R, we can estimate the efficiency with which the absorption is enhanced in a CuPc film over the entire spatial region where the field is enhanced.

The magnitude of the effect integrated over the spectrum, like Q_{NF}, depends on the size of the embedded nanoparticles. In analyzing this dependence, two factors must be taken into account. First, for each wavelength there is an optimal size of silver nanoparticle for which a maximum value of Q_{NF} is attained. Thus, for example, in the transparency region of the matrix (500 nm) the two parameters vary nonmonotonically, reaching a maximum for a particle with a radius of 31 nm, while in the region of maximum absorption (624 nm), there is a slight maximum for
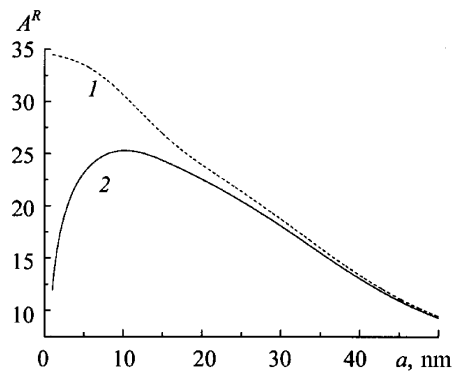
709

Fig. 5. A^R as a function of the radius of spherical nanoparticles embedded in CuPc, neglecting (1) and including (2) the size dependences of the optical constants.

particles with a radius of 10 nm. Second, as the size of the nanoparticles is increased, there is a change in the region of R within which noticeable enhancement of the near field occurs.

In this paper we have taken the size dependences of the optical constants of silver nanoparticles into account. Calculations which neglect the size effects yield both quantitative and qualitative differences in the way A^R varies with the particle size. This is illustrated in Fig. 5, which shows that when the size effects are neglected A^R decreases monotonically with increasing particle size a. When the size effects are taken into account, $A^R(a)$ is nonmonotonic, with a maximum of A_{max}^R for nanoparticles with a radius of 10 nm.

Conclusion. Numerical simulation has been used to study field enhancement and increased energy absorption near the surface of plasmonic nanoparticles embedded in absorbing matrices. It has been shown that the field intensity enhancement near nanoparticles shows up most strongly in the spectral regions where the matrix is transparent. This results in an increase in the fraction of energy absorbed by absorbing matrix materials when nanoparticles are present and also leads to a substantial transformation of its spectral distribution, as illustrated here for the example of copper phthalocyanine with silver nanoparticles. The choice of the size of the plasmonic nanoparticles that are introduced can be used to optimize the absorption in the visible for both the donor and acceptor materials employed in solar cells and, thereby, to increase their energy efficiency.

REFERENCES

1. U. Kreibig and M. Volmer, *Optical Properties of Metal Clusters*, Springer-Verlag, Berlin (1995).
2. B. J. Messinger, K. U. von Raben, R. K. Chang, and P. W. Barber, *Phys. Rev. B*, **24**, 649–657 (1981).
3. M. Quinten, *Appl. Phys. B*, **73**, 245–255 (2001).
4. R. A. Dynich and A. N. Ponyavina, *Zh. Prikl. Spektr.*, **75**, 831–837 (2008).
5. P. Matheu, S. H. Lim, D. Derkac, C. McPheeters, and E. T. Yu, *Appl. Phys. Lett.*, **93**, 121904 (2008).
6. K. Nakayama, K. Tanabe, and H. A. Atwate, *Appl. Phys. Lett.*, **93**, 113108 (2008).
7. C. S. Solanki and G. Beaucarne, *Energy Sustain. Develop.*, **11**, No. 3, 17–23 (2007).
8. W. C. Mundy, J. A. Roux, and A. M. Smith, *J. Opt. Soc. Am.*, **64**, 1593–1597 (1974).
9. P. Chylek, *J. Opt. Soc. Am.*, **67**, 561–563 (1977).
10. C. F. Bohren and D. P. Gilra, *J. Colloid Interface Sci.*, **72**, 215–221 (1979).
11. M. I. Mishchenko, *Opt. Express*, **15**, 13188–13202 (2007).
12. M. Quintem and J. Rostalki, *Part. Part. Syst. Charact.*, **13**, 89–96 (1996).
13. A. N. Lebedev, M. Gartz, U. Kreibig, and O. Stenzel, *Eur. Phys. J. D*, **6**, 365–373 (1999).
14. Q. Fu and W. Sun, *Appl. Opt.*, **40**, 1354–1361 (2001).
15. I. W. Sudiarta and P. Chylek, *J. Opt. Soc. Am. A*, **18**, 1275–1278 (2001).
16. P. B. Johnson and R. W. Christy, *Phys. Rev. B*, **12**, 4370–4387 (1972).
17. L. A. A. Pettersson, L. S. Roman, and O. Inganas, *J. Appl. Phys.*, **86**, 487–496 (1999).